Journal of Applied Sciences

ISSN 1812-5654

science alert

ANSInet
an open access publisher
http://ansinet.com

Journal of Applied Sciences 13 (14): 2819-2824, 2013
ISSN 1812-5654 / DOI: 10.3923/jas.2013.2819.2824

Robot Dynamic Identification Based on the Immune Clonal Selection Algorithm

[1]Liu Haitao and [2]Zhang Tie
[1]Guangdong Ocean University, Zhanjiang, China
[2]South China University of Technology, Guangzhou, China

Abstract: This study deals with the dynamic modeling and excitation trajectory optimization of the RB industrial robot. In the identification, the 6-DOF robot is simplified as the first 3-DOF dynamic model to get the complete dynamic expression and reduced observation matrix and an immune clonal selection algorithm is present to obtain the optimal excitation trajectory to improve the accuracy of dynamic parameters. Simulations show that this optimization algorithm is effective and the accuracy of the estimated parameters directly depends on the selection of excitation trajectory.

Key words: Robot, dynamic identification, immune clonal selection algorithm

INTRODUCTION

Dynamic identification of industrial robot is often required to develop advanced control algorithms. The design of an advanced nonlinear control for industrial robot is usually based on the robot model and its performance directly depends on the model accuracy. Robot identification experiment is the only efficient way to obtain accurate model as well as indications on their accuracy, confidence and validity which deals with the problem of estimating the robot model parameters from the response measured data. In general, a standard robot identification procedure consists of modeling, experiment design, data acquisition, signal processing, parameter estimation and model validation (Swevers *et al*., 2007). Meanwhile, the specially designed experiments are required to ensure the reliability, accuracy and efficiency of identification. Thus, it is essential to consider whether the excitation is sufficient to provide accurate and fast parameter estimation in the presence of disturbances such as measurement noise and actuator disturbances.

Exciting trajectory optimization is a very important procedure to excite all the dynamic parameters and improve the convergence rate and the noise immunity as the robot identification. Jan Swevers *et al*. (1997) proposed a stochastic framework to optimize the excitation trajectory. Due to the complexity of the optimization problem, a genetic algorithm is often used to solve the above optimization problem. Vuong and Ang Jr (2009) present a genetic algorithm to solve the trajectory optimization problem. But the genetic algorithm is easily prone to premature, into a local optimum value. Therefore, Based on the fact that immune clonal selection algorithm has better ability both at overall and partial searching than genetic algorithm, we introduce the excitation trajectory optimization method based on the clonal selection algorithm.

Immune Clonal Selection Algorithm (ICSA), is one of intelligent algorithms that being brought forward from immune conception and theory in life sciences. It is a excellent parallel and heuristic optimization algorithm (Campelo *et al*., 2005; Chun *et al*., 1997; De Castro and Von Zuben, 2002) that the clonal selection mechanism of the immune system is introduced into simple search algorithm.

DYNAMIC MODEL OF THE RB ROBOT

An accurate dynamic model is important for model-based control of robot. The RB industrial robot and its coordinate frames are shown in Fig. 1. The Denavit Hartenberg parameters of the robot are given in Table 1.

The dynamic model of RB robot can be derived from the Lagrange-Euler formulation. It is commonly written as:

$$H(q)\ddot{q} + C(q,\dot{q})\dot{q} + G(q) = \tau \quad (1)$$

where, $q, \dot{q}, \ddot{q} \in R^n$ denotes the position, velocity and acceleration, respectively, H(q) is a symmetric, positive definite inertia matrix, $C(q,\dot{q}) \in R^{n\times n}$ denotes the centrifugal and Coriolis matrix, $G(q) \in R_n$ is the gravity term and $\tau \in R_n$ denotes the torque input vector. In practice, the six degrees of freedom industrial robot dynamics equation is quite complex, so it is not realistic to calculate its complete expression. Taking into account the special structure of the robot: Three wrist joints are perpendicular to each other to mainly adjust the end-effector attitude of the robot and the dynamic parameter values (including

Corresponding Author: Liu Haitao, Guangdong Ocean University, Zhanjiang, China

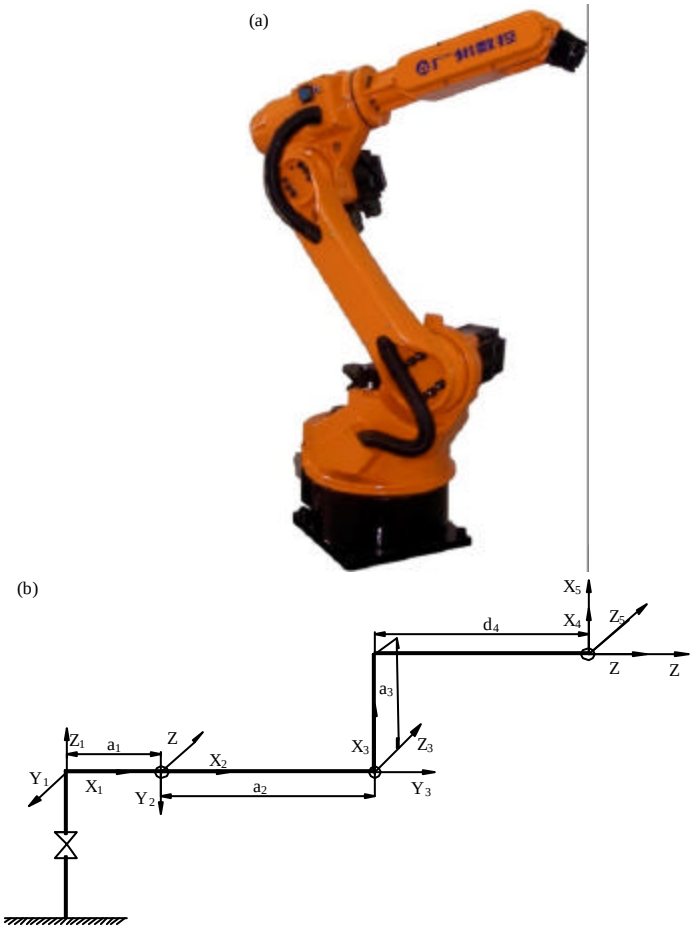

Fig. 1(a-b): RB industrial robot (a) The RB industrial robot (b) The D-H Frames

Table 1: D-H parameters for RB robot

i	α_{i-1}	a_{i-1}	d_i	q_i
1	0	0	0	q_1
2	-π/2	a_1	0	q_2
3	0	a_2	0	q_3
4	-π/2	a_3	d_4	q_4
5	π/2	0	0	q_5
6	-π/2	0	0	q_6

quality, inertia, inertia, etc.) are relatively smaller; while the previous three links are to achieve the location of the end-effector and the dynamic parameters are larger, so nonlinear effect is quite significant, especially the gravity impacts of the second and third joints are particularly apparent. Therefore, the robot dynamics of the first three links are only considered in this study and the dynamics of the wrist joints as external disturbances. Som as to reduce the computational complexity on the one hand, on the other hand to reduce the parameters to be identified which easily obtain relatively accurate dynamic model.

The dynamics of the first three links of a six-DOF RB robot can be modeled by:

$$\begin{bmatrix}\tau_1\\ \tau_2\\ \tau_3\end{bmatrix}=\begin{bmatrix}h_{11} & h_{12} & h_{13}\\ h_{21} & h_{22} & h_{23}\\ h_{31} & h_{32} & h_{33}\end{bmatrix}\begin{bmatrix}\ddot{q}_1\\ \ddot{q}_2\\ \ddot{q}_3\end{bmatrix}+\begin{bmatrix}c_{11} & c_{12} & c_{13}\\ c_{21} & c_{22} & c_{23}\\ c_{31} & c_{32} & c_{33}\end{bmatrix}\begin{bmatrix}\dot{q}_1\\ \dot{q}_2\\ \dot{q}_3\end{bmatrix}+\begin{bmatrix}g_1\\ g_2\\ g_3\end{bmatrix} \quad (2)$$

The elements of the mass matrix are as the following:

$$\begin{aligned}
h_{11} &= I_{1zz}+\frac{1}{2}\left(I_{2xx}+I_{2yy}+I_{3xx}+I_{3yy}-I_{3xx}c2_{23}+I_{3yy}c2_{23}\right)\\
&\quad -I_{3xy}s2_{23}+a_1^2\left(m_2+m_3\right)+\frac{1}{2}\left(a_2^2m_3-I_{2xx}c2_2+I_{2yy}c2_2\right)\\
&\quad -I_{2xy}s2_2+\frac{1}{2}a_2^2m_3c2_2+2a_1m_3r_{3x}c_{23}-2a_1m_3r_{3y}s_{23}\\
&\quad +2a_1a_2m_3c_2+2a_1m_2r_{2x}c_2+a_2m_3r_{3x}c_3-2a_1m_2r_{2y}s_2\\
&\quad -a_2m_3r_{3y}s_3+a_2m_3\left(r_{3x}c_32_2-r_{3y}s_32_2\right)\\
h_{12} &= I_{3yz}c_{23}+I_{3xz}s_{23}+I_{2yz}c_2+I_{2xz}s_2+a_2m_3r_{3z}s_2\\
h_{13} &= I_{3yz}c_{23}+I_{3xz}s_{23}\\
h_{22} &= I_{2zz}+I_{3zz}+a_2^2m_3+2a_2m_3\left(r_{3x}c_3-r_{3y}s_3\right)\\
h_{23} &= I_{3zz}+a_2m_3\left(r_{3x}c_3-r_{3y}s_3\right)\\
h_{33} &= I_{3zz}
\end{aligned}$$

$$c_{11} = -\dot{q}_2(I_{3xy}c2_{23} - \frac{1}{2}I_{3xx}s2_{23} + \frac{1}{2}I_{3yy}s2_{23} + I_{2xy}c2_2 - \frac{1}{2}I_{2xx}s2_2 + \frac{1}{2}I_{2yy}s2_2 + \frac{1}{2}a_2^2m_3s2_2 + a_1m_3r_{3y}c_{23} + a_1m_3r_{3x}s_{23} + a_1a_2m_3s_2 + a_1m_2r_{2y}c_2 + a_1m_2r_{2x}s_2 + a_2m_3r_{3y}c_3 2_2 + a_2m_3r_{3x}s_3 2_2) - \dot{q}_3(I_{3xy}c2_{23} - \frac{1}{2}I_{3xx}s2_{23} + \frac{1}{2}I_{3yy}s2_{23} + a_1m_3r_{3y}c_{23} + a_1m_3r_{3x}s_{23} + \frac{1}{2}a_2m_3r_{3y}c_3 + \frac{1}{2}a_2m_3r_{3x}s_3 + \frac{1}{2}a_2m_3r_{3y}c_3 2_2 + \frac{1}{2}a_2m_3r_{3x}s_3 2_2)$$

$$c_{12} = \dot{q}_2(I_{3xz}c_{23} - I_{3yz}s_{23} + I_{2xz}c_2 - I_{2yz}s_2 + a_2m_3r_{3z}c_2) - \dot{q}_1(I_{3xy}c2_{23} - \frac{1}{2}I_{3xx}s2_{23} + \frac{1}{2}I_{3yy}s2_{23} + I_{2xy}c2_2 - \frac{1}{2}I_{2xx}s2_2 + \frac{1}{2}I_{2yy}s2_2 + \frac{1}{2}a_2^2m_3s2_2 + a_1m_3r_{3y}c_{23} + a_1m_3r_{3x}s_{23} + a_1a_2m_3s_2 + a_1m_2r_{2y}c_2 + a_1m_2r_{2x}s_2 + a_2m_3r_{3y}c_3 2_2 + a_2m_3r_{3x}s_3 2_2) + \dot{q}_3(I_{3xz}c_{23} - I_{3yz}s_{23})$$

$$c_{13} = \dot{q}_2(I_{3xz}c_{23} - I_{3yz}s_{23}) - \dot{q}_1(I_{3xy}c2_{23} - \frac{1}{2}I_{3xx}s2_{23} + \frac{1}{2}I_{3yy}s2_{23} + a_1m_3r_{3y}c_{23} + a_1m_3r_{3x}s_{23} + \frac{1}{2}a_2m_3r_{3y}c_3 + \frac{1}{2}a_2m_3r_{3x}s_3 + \frac{1}{2}a_2m_3r_{3y}c_3 2_2 + \frac{1}{2}a_2m_3r_{3x}s_3 2_2) + \dot{q}_3(I_{3xz}c_{23} - I_{3yz}s_{23})$$

$$c_{21} = \dot{q}_1(I_{3xy}c2_{23} - \frac{1}{2}I_{3xx}s2_{23} + \frac{1}{2}I_{3yy}s2_{23} + I_{2xy}c2_2 - \frac{1}{2}I_{2xx}s2_2 + \frac{1}{2}I_{2yy}s2_2 + \frac{1}{2}a_2^2m_3s2_2 + a_1m_3r_{3y}c_{23} + a_1m_3r_{3x}s_{23} + a_1a_2m_3s_2 + a_1m_2r_{2y}c_2 + a_1m_2r_{2x}s_2 + a_2m_3r_{3y}c_3 2_2 + a_2m_3r_{3x}s_3 2_2)$$

$$c_{22} = -\dot{q}_3a_2m_3(r_{3y}c_3 + r_{3x}s_3)$$

$$c_{23} = -\dot{q}_2a_2m_3(r_{3y}c_3 + r_{3x}s_3) - \dot{q}_3a_2m_3(r_{3y}c_3 + r_{3x}s_3)$$

$$c_{31} = \dot{q}_1(I_{3xy}c2_{23} - \frac{1}{2}I_{3xx}s2_{23} + \frac{1}{2}I_{3yy}s2_{23} + a_1m_3r_{3y}c_{23} + a_1m_3r_{3x}s_{23} + \frac{1}{2}a_2m_3r_{3y}c_3 + \frac{1}{2}a_2m_3r_{3x}s_3 + \frac{1}{2}a_2m_3r_{3y}c_3 2_2 + \frac{1}{2}a_2m_3r_{3x}s_3 2_2) \backslash$$

$$c_{32} = \dot{q}_2a_2m_3(r_{3y}c_3 + r_{3x}s_3)$$

$$c_{33} = 0$$

$$g_1 = 0$$

$$g_2 = gm_3r_{3x}c_{23} - gm_3r_{3y}s_{23} + a_2gm_3c_2 + gm_2r_{2x}c_2 - gm_2r_{2y}s_2$$

$$g_3 = gm_3r_{3x}c_{23} - gm_3r_{3y}s_{23}$$

where, c_3 = cosq$_3$, s_3 = sinq$_3$, c_{23} = cos(q_2+q_3), s_{23} = sin(q_3+q_3), $c2_{23}$ = cos(2q_2+2q_3), $s2_{23}$ = sin(2q_2+2q_3), c_32_2 = cos(2$_{q2}$+q_3) s_32_2 = sin(2$_{q2}$+q_3) the acceleration of gravity.

In order to reduce the system complexity, Eq. 2 can also be rewritten linearly in terms of the physical parameters of the system. it is impossible to estimate all the link dynamic parameter values from the data of link motions and joint torques or forces since the link dynamic parameters are redundant to determine the dynamic model uniquely. So a set of dynamic parameters are called base dynamic parameters or minimum dynamic parameters which is sufficient to describe the dynamic behavior of the mechanical system along with the reduced observation matrix (Mayeda *et al*., 1990). Therefore, the base dynamic parameter in linear form is given as following:

Table 2: Minimum inertia parameters

Parameters	Meaning	Unit
θ_1	$I_{1zz}+I_{2yy}+I_{3yy}+a^2{}_2m_3+a_1{}^2(m_2+m_3)$	kg m^2
θ_2	$I_{2xx}-I_{2yy}-a^2{}_2m_3$	kg m^2
θ_3	I_{2xy}	kg m^2
θ_4	$I_{2xz}+a_2m_3r_{3z}$	kg m^2
θ_5	I_{2yz}	kg m^2
θ_6	$I_{2zz}+a_2{}^2m_3$	kg m^2
θ_7	$m_2r_{2x}+a_2m_3$	kg m
θ_8	m_2r_{2y}	kg m
θ_9	$I_{3xx}-I_{3yy}$	kg m^2
θ_{10}	I_{3xy}	kg m^2
θ_{11}	I_{3xz}	kg m^2
θ_{12}	I_{3yz}	kg m^2
θ_{13}	I_{3zz}	kg m^2
θ_{14}	m_3r_{3x}	kg m
θ_{15}	m_3r_{3y}	kg m

$$\tau = \Phi(q,\dot{q},\ddot{q})\theta \tag{3}$$

where, $\theta = [\theta_1, \theta_2, \cdots \theta_{15}]_T$ is the minimum dynamic parameters vector. These elements in θ is given in Table 2. $\Phi(q,\dot{q},\ddot{q})$ is observation matrix as:

$$\Phi = \begin{bmatrix} \varphi_{11}, \varphi_{12}, \cdots, \varphi_{115} \\ \varphi_{21}, \varphi_{22}, \cdots, \varphi_{215} \\ \varphi_{31}, \varphi_{32}, \cdots, \varphi_{315} \end{bmatrix} \tag{4}$$

where the elements of Φ are given in Appendix A. a_1 = 0.1 m, a_2 = 0.25 m; m_1, m_2, m_3 are the masses of link 1, 2, 3, respectively; I_{1xx}, I_{1yy}, I_{1zz} are the three-axis moments of inertia for link 1, respectively. I_{1xy}, I_{1yz}, I_{1xz} are the three-axis poles of inertia for link 1, respectively. r_{c1}= [r_{1x}, r_{1y}, r_{1z}] is the coordinate expression in the Department of (Nusawardhana, 2007). Link 2 and 3 are similar with so.

EXCITATION TRAJECTORY OPTIMIZATION

In order to improve the convergence rate and the noise immunity of the least squares estimation, the trajectory used to get observation data must be carefully selected. Therefore, a persistently exciting trajectory satisfying some optimization criteria is calculated by some intelligent algorithms, such as particle swarm optimization algorithm, genetic algorithm.

The convergence rate and noise immunity of a parameter identification experiment depend directly upon the condition number of the persistent excitation matrix computed from the inverse dynamic model, since the condition number represents an upper limit for input/output error transmissibility (Gautier and Khalil, 1992), i.e., the configurations for which measurements are taken must correspond to a well-conditioned reduced observation matrix. Therefore, we select the following optimization criteria:

$$J = k_1\text{cond}(\Phi) + k_2\frac{1}{\sigma_{min}} \tag{5}$$

where $k_1>0$, $k_2>0$ are the weighting scalar parameters representing the relative weights between the condition number of the observation matrix: cond(Φ) and its minimum singular value: σ_{min}.

The exciting trajectory is selected as the periodic trajectory which can be parameterized as a sum of finite Fourier series (6) and is adopted because of their advantages in terms of signal processing (Swevers *et al*., 1997).

$$\begin{aligned} q_i(t) &= q_{i0} + \sum_{l=1}^{N} a_l^i \sin(w_f lt) - b_l^i \cos(w_f lt) \\ \dot{q}_i(t) &= \sum_{l=1}^{N} a_l^i w_f l \cos(w_f lt) + b_l^i w_f l \sin(w_f lt) \\ \ddot{q}_i(t) &= \sum_{l=1}^{N} -a_l^i (w_f l)^2 \sin(w_f lt) + b_l^i (w_f l)^2 \cos(w_f lt) \end{aligned} \quad (6)$$

where w_f is the fundamental frequency of the excitation trajectories and should be carefully chosen not to excite the un-modeled dynamics of the robot. l = 1, 2,…,N, Ceach Fourier series contains 2N+1parameters. The problem of finding the optimal trajectory becomes determining the coefficients (q_{i0}, a_k^i, b_k^i) in order to minimize the cost function (5). Due to the joint position, velocity, acceleration of the robot are bounded, the above optimization problem is complex multi-constraint optimization problem, a good initial guess for this optimization is hard to achieve. Thus, an Immune Clonal Algorithm is proposed to solve the above optimization problem in this study.

The Clonal selection algorithm (De Castro and Von Zuben, 2000) takes full advantage of the diversity mechanisms of the immune system and has a very superior ability of global optimization. So the excitation trajectory optimization procedure is as follows:

Step 1: Generate a set (P) of candidate solutions, composed of the subset of memory cells (M) and the remaining population Pr, i.e., P = M+Pr

Step 2: Select the n best individuals of the population (Pn), based on an affinity measure

Step 3: Clone these n best individuals of the population, giving rise to a temporary population of clones (C). The clone size is an increasing function of the affinity with the antigen

Step 4: Submit the population of clones to a hypermutation scheme, where the hypermutation is proportional to the affinity of the antibody with the antigen. A maturated antibody population is generated (C*)

Step 5: Re-select the improved individuals from C* to compose the memory set M. Some members of P can be replaced by other improved members of C*

Step 6: Replace d antibodies by novel ones (diversity introduction). The lower affinity cells have higher probabilities of being replaced

Step 7: Return Step 2 to continue the cycle calculation, until the termination conditions.

SIMULATION

In order to illustrate the validity of the excitation trajectory optimization based the clonal selection algorithm (CSA), the simulation on the RB robot dynamics is considered. In the simulation, the excitation trajectory is the desired input signal, the traditional PD control method is used and the actually required control torque is calculated according to the robot dynamic model. In addition, the white Gaussian noise is introduced as the measurement interference signal to verify the robustness of the identification method.

The optimization constraints are as follows:

- **The joint position ranges (rad):** $-\pi<q_1<\pi$, $-7\pi/18<q_2<7\pi/18$, $-\pi/4<q_3<\pi/4$
- **The joint velocity ranges (rad/s):** $-2\pi<q_1<2\pi$, $-2\pi<q_2<2\pi$, $-2\pi<q_3<2\pi$
- **The joint acceleration ranges(rad/s^2):** $-2\pi<\ddot{q}_1<2\pi$, $-2\pi<\ddot{q}_2<2\pi$, $-2\pi<\ddot{q}_3<2\pi$

Define $w_f = 2$, when N = 1, there are nine optimization parameters. Set the initial population of 50, good population of 10 and 200 iterations, the iterative result is shown in Table 3.

In the following, The feasibility of the excitation trajectory optimization is present by the parameter estimation and model validation and compared with un-optimized trajectory:

$$\begin{aligned} q_1(t) &= q_2(t) = q_3(t) = \sin(2t) \\ \dot{q}_1(t) &= \dot{q}_2(t) = \dot{q}_3(t) = 2\cos(2t) \\ \ddot{q}_1(t) &= \ddot{q}_2(t) = \ddot{q}_3(t) = -4\sin(2t) \end{aligned} \quad (7)$$

Both of the above excitation trajectories are employed to get the observation data and dynamic parameters are estimated by the least squares method. The estimated results are as shown in Table 4. Estimation 1 is the estimated results by using the un-optimized trajectory while estimation 2 by using the optimized trajectory. In order to compare the accuracy of the

Table 3: Trajectory parameters optimization results

Parameters	q_{10}	a_1^1	b_1^1	q_{20}	a_1^2	b_1^2
Values	0.1658	0.9077	0.4732	0.0806	0.4594	0.4917
Parameters	q_{30}	a_1^3	b_1^3			
Values	0.3140	0.1251	0.4840			
Affinity	72.97					

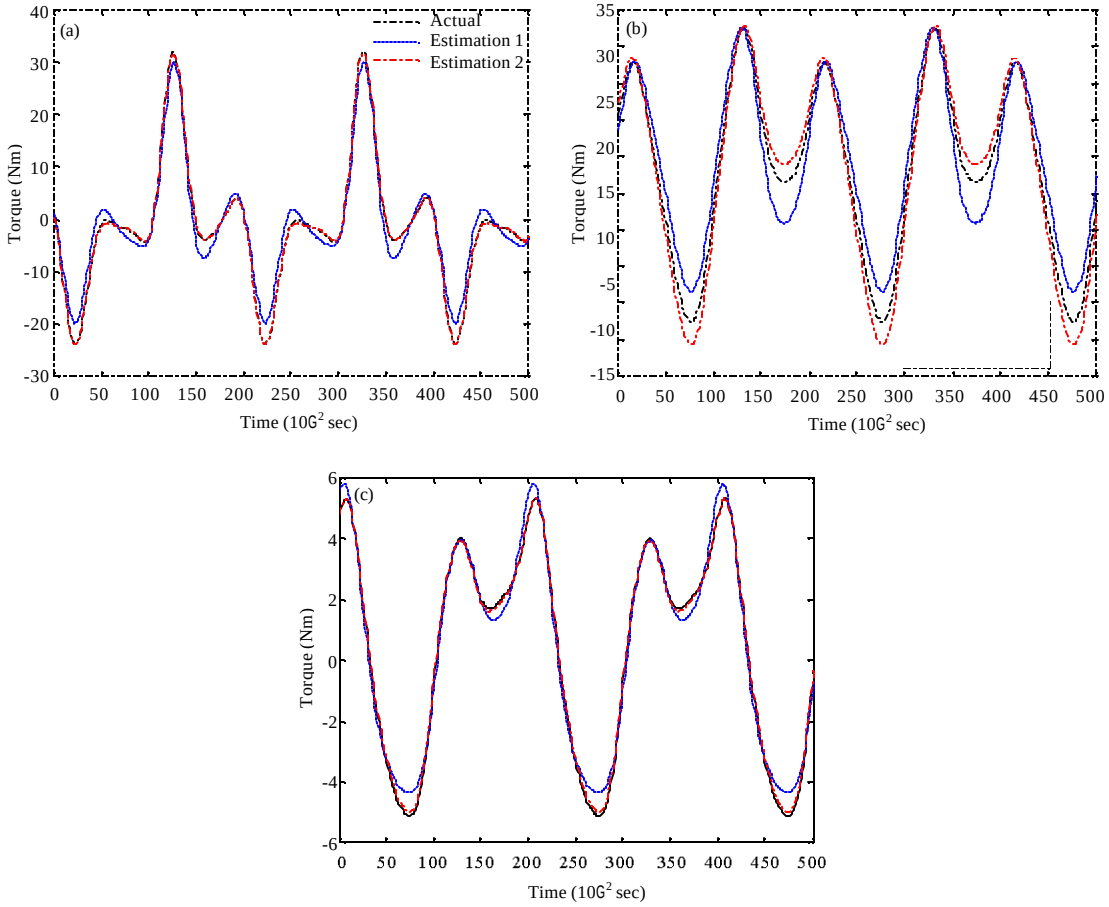

Fig. 2: Model validation

Table 4: Parameters estimation results

Parameters	Actual	Estimation 1	Estimation 2
θ_1 (kg m^2)	1.2804	1.0462	1.2675
θ_2 (kg m^2)	-0.6508	-0.6516	-0.6232
θ_3 (kg m^2)	0.0173	0.0705	0.0348
θ_4 (kg m^2)	0.1258	0.1518	0.1220
θ_5 (kg m^2)	0.0083	-0.0126	0.0141
θ_6 (kg m^2)	0.6957	0.6449	0.9840
θ_7 (kg m)	2.6843	2.8411	2.6822
θ_8 (kg m)	0.1469	-0.1846	0.0179
θ_9 (kg m^2)	-0.0125	0.0670	-0.0180
θ_{10} (kg m^2)	0.0251	0.0147	0.0214
θ_{11} (kg m^2)	0.0058	0.0225	0.0070
θ_{12} (kg m^2)	0.0053	0.0011	0.0050
θ_{13} (kg m^2)	0.0768	0.0748	0.0686
θ_{14} (kg m)	0.2752	0.2638	0.2761
θ_{15} (kg m)	0.2208	0.2407	0.2253

estimation results, a trajectory different from the excitation trajectory in identification is planned for model validation:

$$\begin{cases} q_1 = \sin(\pi t) + \cos(\pi t) \\ q_2 = \sin(\pi t) - \cos(\pi t) \\ q_3 = \sin(\pi t) \end{cases} \quad (8)$$

The identification parameter values are substituted into the robot dynamic model to calculate the estimated drive torques. In addition, the actual drive torques are calculated based on the actual parameters. Compared the actual and estimated drive torque, is to judge the accuracy of the robot identification parameters. The model validation results are shown in Fig. 2, we easily see that the estimation 2 (dash-dotted line) are better than estimation 1(dotted line) which shows that the dynamic parameters using optimal trajectory are more accurate than un-optimal trajectory.

CONCLUSION

In this study, the immune clonal selection algorithm was used to optimize the excitation trajectory to improve the accuracy and robustness of the parameters identification for the RB robot. The first three links dynamics of the RB robot are only considered, so the minimum dynamic parameters and the reduced

observation matrix are completely obtained. To verify the optimization results, we present the identification simulation on the RB robot. The identification results show that the accuracy of the estimated inertial parameters directly depends on the selection of efficient excitation trajectory. The next study is the identification experiments of the RB robot.

APPENDIX

Appendix A. Elements of the observation matrix:

$$\varphi_{11} = \ddot{q}_1$$
$$\varphi_{12} = \ddot{q}_1 s_2^2 + \dot{q}_1\dot{q}_2 s2_2$$
$$\varphi_{13} = -\ddot{q}_1 s2_2 - 2\dot{q}_1\dot{q}_2 c2_2$$
$$\varphi_{14} = \ddot{q}_2 s_2 + \dot{q}_2^2 c_2$$

$$\varphi_{15} = \ddot{q}_2 c_2 - \dot{q}_2^2 s_2$$
$$\varphi_{16} = 0$$
$$\varphi_{17} = 2a_1(\ddot{q}_1 c_2 - \dot{q}_1\dot{q}_2 s_2)$$
$$\varphi_{18} = -2a_1(\ddot{q}_1 s_2 - \dot{q}_1\dot{q}_2 c_2)$$
$$\varphi_{19} = -\frac{1}{2}\ddot{q}_1 c2_{23} + \dot{q}_1(\dot{q}_2 + \dot{q}_3)s2_{23}$$
$$\varphi_{110} = -\ddot{q}_1 s2_{23} - 2\dot{q}_1(\dot{q}_2 + \dot{q}_3)c2_{23}$$
$$\varphi_{111} = (\ddot{q}_2 + \ddot{q}_3)s_{23} + (\dot{q}_2 + \dot{q}_3)^2 c_{23}$$
$$\varphi_{112} = (\ddot{q}_2 + \ddot{q}_3)c_{23} - (\dot{q}_2 + \dot{q}_3)^2 s_{23}$$
$$\varphi_{113} = 0$$
$$\varphi_{114} = \ddot{q}_1(a_2c_3 + a_2c_32_2 + 2a_1c_{23}) - 2\dot{q}_1\dot{q}_2(a_2s_32_2 + a_1s_{23}) - \dot{q}_1\dot{q}_3(2a_1s_{23} + a_2s_3 + a_2s_32_2)$$
$$\varphi_{115} = -\ddot{q}_1(a_2s_3 + a_2s_32_2 + 2a_1s_{23}) - 2\dot{q}_1\dot{q}_2(a_2c_32_2 + a_1c_{23}) - \dot{q}_1\dot{q}_3(2a_1c_{23} + a_2c_3 + a_2c_32_2)$$

$$\varphi_{21} = 0$$
$$\varphi_{22} = -\dot{q}_1^2 s_2 c_2$$
$$\varphi_{23} = \dot{q}_1^2 c2_2$$
$$\varphi_{24} = \ddot{q}_1 s_2$$
$$\varphi_{25} = \ddot{q}_1 c_2$$
$$\varphi_{26} = \ddot{q}_2$$
$$\varphi_{27} = \dot{q}_1^2 a_1 s_2 + g c_2$$
$$\varphi_{28} = \dot{q}_1^2 a_1 c_2 - g s_2$$
$$\varphi_{29} = -\dot{q}_1^2 s_{23} c_{23}$$
$$\varphi_{210} = \dot{q}_1^2 c2_{23}$$
$$\varphi_{211} = \ddot{q}_1 s_{23}$$
$$\varphi_{212} = \ddot{q}_1 c_{23}$$
$$\varphi_{213} = \ddot{q}_2 + \ddot{q}_3$$
$$\varphi_{214} = (2\ddot{q}_2 + \ddot{q}_3)a_2c_3 - a_2s_3(2\dot{q}_2 + \dot{q}_3)\dot{q}_3 + (a_1s_{23} + a_2s_32_2)\dot{q}_1^2 + gc_{23}$$
$$\varphi_{215} = -(2\ddot{q}_2 + \ddot{q}_3)a_2s_3 - a_2c_3(2\dot{q}_2 + \dot{q}_3)\dot{q}_3 + (a_1c_{23} + a_2c_32_2)\dot{q}_1^2 - gs_{23}$$
$$\varphi_{39} = -\ddot{q}_1 s_{23} c_{23}$$
$$\varphi_{310} = \dot{q}_1^2 c2_{23}$$
$$\varphi_{311} = \ddot{q}_1 s_{23}$$
$$\varphi_{312} = \ddot{q}_1 c_{23}$$
$$\varphi_{313} = \ddot{q}_2 + \ddot{q}_3$$
$$\varphi_{314} = \ddot{q}_2 a_2 c_3 + \dot{q}_1^2(a_1s_{23} + a_2s_{23}c_2) + \dot{q}_2^2 a_2 s_3 + g c_{23}$$
$$\varphi_{315} = -\ddot{q}_2 a_2 s_3 + \dot{q}_1^2\left[a_1c_{23} + \frac{1}{2}a_2(c_3 + c_32_2)\right] + \dot{q}_2^2 a_2 c_3 - g s_{23}$$

The other elements are zero.

ACKNOWLEDGMENTS

The study was supported by the National High-Technology Research and Development Program ("863" Key Program 2009AA043901-3), the Science and Technology Planning Project of Zhanjiang City (2012A0103).

REFERENCES

Campelo, F., F.G. Guimaraes, H. Igarashi and J.A. Ramirez, 2005. A clonal selection algorithm for optimization in electromagnetics. IEEE Trans. Magnetics, 41: 1736-1739.

Chun, J.S., M.K. Kim, H.K. Jung and S.K. Hong, 1997. Shape optimization of electromagnetic devices using immune algorithm. IEEE Trans. Magn., 33: 1876-1879.

De Castro, L.N. and F. von Zuben, 2002. Learning and optimization using the clonal selection principle. IEEE Trans. Evolut. Comput., 6: 239-251.

De Castro, L.N. and F.J. von Zuben, 2000. The clonal selection algorithm with engineering applications. Proceedings of the Conference on Genetic and Evolutionary Computation, Workshop on Artificial Immune Systems and their Applications, July 2000, Las Vegas, USA., pp: 36-37.

Gautier, M. and W. Khalil, 1992. Exciting trajectories for the identification of base inertial parameters of robots. Int. J. Robotics Res., 11: 362-375.

Mayeda, H., K. Yoshida and K. Osuka, 1990. Base parameters of manipulator dynamic models. IEEE Trans. Robotics Automation, 6: 312-321.

Nusawardhana, A., 2007. Nonlinear synergetic optimal controllers. American Institute of Aeronautics and Astronautics, ETATS-UNIS, Reston, VA.

Swevers, J., C. Ganseman and D.B. Tukel, 1997. Optimal robot excitation and identification. IEEE Trans. Robotics Automation, 13: 730-740.

Swevers, J., W. Verdonck and J. de Schutter, 2007. Dynamic model n for industrial robots. IEEE Control Syst. Magazine, 27: 58-71.

Vuong, N.D. and M.H. Ang Jr, 2009. Dynamic model identification for industrial robots. Acta Polytechnica Hungarica, 6: 51-68.